Physica Scripta

PAPER • OPEN ACCESS

Viscous fluid with neutrino in f(R,Φ,X) gravity

To cite this article: Erkan Eraslan *et al* 2025 *Phys. Scr.* **100** 075227

Physica Scripta

CrossMark

OPEN ACCESS

RECEIVED
4 March 2025

REVISED
6 May 2025

ACCEPTED FOR PUBLICATION
4 June 2025

PUBLISHED
16 June 2025

PAPER

Viscous fluid with neutrino in f(R,Φ,X) gravity

Erkan Eraslan[1], **Melis Ulu Doğru**[2], **Doğukan Taşer**[3,*] **and Hüseyin Aydın**[4]

[1] Department of Physics, School of Graduate Studies, Çanakkale Onsekiz Mart University, 17020, Çanakkale, Turkey
[2] Department of Physics, Science Faculty, Çanakkale Onsekiz Mart University, 17020, Çanakkale, Turkey
[3] Department of Electricity and Energy, Çan Vocational School, Çanakkale Onsekiz Mart University, 17400, Çanakkale, Turkey
[4] State Hydrolic Works (DSI), 61220, Trabzon, Turkey
[*] Author to whom any correspondence should be addressed.

E-mail: erkan.eraslan@comu.edu.tr, melisulu@comu.edu.tr, dogukantaser@comu.edu.tr and huseynaydin@gmail.com

Keywords: Kantowski-Sachs universe, neutrino, f(R,Φ,X) gravity, energy conditions

Abstract

In this study, we investigate the Kantowski-Sachs space-time within the framework of f(R,Φ,X) gravity, incorporating a general fluid distribution with neutrino contributions. The field equations are constructed using a hybrid f(R,Φ,X) function that combines features of the Starobinsky-like model and k-essence functions with canonical scalar fields. Analytical solutions are obtained, showing that the fluid can exhibit bulk viscous behavior with neutrino contributions. The model's kinematical properties and energy conditions are investigated. NEC, WEC and DEC are satisfied, while SEC is violated, indicating scenarios where gravity repels matter, enabling exotic configurations. These results provide insights into the early universe's dynamics and the role of viscous fluids and neutrinos in modified gravity theories.

1. Introduction

Observations of large-scale galaxies point that cosmic matter in the present Universe could be described by a perfect fluid. Furthermore, instabilities during which galaxies are formed suggest that the fluid behaves like a viscous fluid [1]. Cosmological models for early stages are associated with viscous fluid because they include initial irregularities [2]. Cosmological models in Bianchi Type-I universe were investigated for viscous fluid consisting of mass and shear viscosity. It has been shown how important dynamics of shear and fluid density change during evolution [3]. Effect of time-dependent mass viscosity in Friedmann-Robertson-Walker universe with Brans-Dicke theory is examined [4]. By modeling with fixed deceleration parameters, solutions were obtained for inflationary period of the Universe and a period dominated by radiation [4]. They investigated shear and LRS Bianchi Type-I space-time string dust magnetized cosmological model in General Relativity under some conditions. Using assumption that sheer and expansion are directly proportional to obtain a specific solution, it has been discussed [5]. With the extended irreversible thermodynamics approach, an equivalent formulation of equations is provided in the case of bulk viscosity by making an appropriate change in variables. It is also shown that this model provides new ways to directly calculate bulk viscosity. Concrete examples are presented to establish the Israel-Stewart model for general volumetric viscous fluid [6]. In order to study about accelerated expansion of the Universe in f(Q) modified gravity, a cosmological model dominated by mass viscous matter was considered, with the mass viscosity coefficient proportional to the speed and acceleration of the expanding universe. Then, compatible values of model parameters were obtained and compared with current observation data [7]. In alternative gravitational theories, many models including bulk viscosity were examined from different aspects [8–10].

Observations impose on us the necessity of determining cosmological parameters precisely. To improve the current standard cosmological model and its alternatives, it is necessary to make very precise cosmological parameter adjustments. All available observations are consistent with the simplest Λ-Cold Dark Matter (Λ-CDM) model. However, since the current model cannot explain some of mysterious cosmological components such as dark matter and dark energy, this model is only a convenient template of the Universe.

Therefore, in order to perceive the functioning of the Universe, precisely determined parameters are needed, structures that can both meet standard expectations and verify effects that have not yet been detected. Models about effect and the evolution of neutrino, one of these structures, on the Universe are of great importance. The Big Bang theory is that cosmic neutrinos left us with remnants to this day. Although this cosmic background remnant has not yet been detected, compatible results have been obtained by some indirect means [11–15]. In f(R) modified gravitation theory, as an alternative cosmology to the Λ-CDM model, it has been shown that effect of large-mass neutrinos on the matter power spectrum, the anomalous growth of density fluctuations on small scales due to scalaron force, can be compensated by the free flow of neutrinos [16]. Using the latest observations from cosmic microwave background (CMB) and baryon acoustic oscillation (BAO) measurements, neutrino properties are constrained in f(R) gravitation theory. First of all, the total mass of neutrinos and effective number of neutrino types were limited. These parameters were then constrained simultaneously and compared with Planck CMB data, WMAP CMB polarization data, BAO data, and data from the Atacama Cosmology Telescope and the South Pole Telescope [17].

Although standard cosmology and Einstein's Gravitation theory give results compatible with observations, they cannot fully explain some cosmological substitutions. At this point, alternative gravity theories have the potential to offer a comprehensive or at least a specific explanation for some of these situations. Recently, f(R)-type theories, one of alternative gravity theories, have been studied quite intensively. Each of these theories provides many strong or weak features due to the parameters they contain and the models they create. Increasing the number of parameters of alternative gravity theory and introducing new features often causes the theory to become more complex and difficult to analyze. For this reason, the creation of an alternative gravity theory involves a very balanced set of choices. In this context, f(R,Φ,X) alternative gravity theory contained in this study is an important theory in terms of parameter diversity and scope it contains. For first time, cosmological perturbations, slow-roll inflation and vacuum state quantum fluctuations were investigated for the generalized gravitation theory including tachyonic condensation within the frame of f(R,Φ,X) theory [18]. It is associated with coupled dark energy scenarios in Einstein-Frame, considering a model with Lagrangian density f = F(Φ)R +2p(Φ,X). Additionally, conformal rotational perturbation equations were derived. We also examined the evolution of perturbations in both the Jordan-Frame and Einstein-Frame in the case where the energy fraction of dark energy is constant in a matter-dominated epoch [19]. In f(R,Φ,X) theory, which is a generalized alternative theory of gravity, various dark energy, and alternative gravity models have been put forward, and models and applications within this theory have been examined for the recent accelerated expansion of the Universe [20]. For k-essence and f(R) gravitation theory, phase space in a vacuum state has been examined in detail. Their proposed model has been shown to be a useful way of explaining inflation period in the early-time universe. It has also been shown that the developed model has a mathematical structure that supports expansion in radiation and matter-dominated periods and is also successful for canonical and ghost scalar fields [21].

The motivation of this study is to compare and discuss bulk viscous fluid with neutrinos in the context of f(R,Φ,X) gravity via Kantowski-Sachs space-time, which depicts the early-time of the Universe. It also aims to demonstrate the compatibility of the developed models and distributions with observational data.

This article includes the contents as follows: In section 2, we mention widely-known alternative gravitation theories. One of the theories, f(R,Φ,X) gravity, is presented with general properties about action function and field equations. In section 3, we get Kantowski-Sachs space-time, their field equations and solutions with general fluid distribution in the context of f(R,Φ,X) gravity. Average scale factor, Hubble parameter, anisotropy parameter and deceleration parameter of the constructed model are calculated and discussed. It is shown that obtained solutions in f(R,Φ,X) gravity sign that considered general fluid could be viscous fluid with neutrinos. Effective matter distributions and energy conditions of them are obtained. All obtained results are examined in terms of physical meaning and geometrical properties in the Conclusion section.

2. Modified gravitation theories

Many alternative gravity theories have been put forward. Of these, f(R)-type theories are still up to date. f(R) theory includes f(R) function instead of Ricci scalar (R) in action integral [22]. f(R,Φ) theory is obtained by adding scalar field (Φ) which originates from the potential energy of matter, to f(R) function in f(R) theory [23]. K-essence theory, which focuses on explaining early-time inflation and late-time expansion of the Universe and tries to explain inflation dynamics of the Universe with negative pressure, was put forward [24]. Finally, f(R,Φ,X) theory emerges as a hybrid alternative gravity theory formed by the combination of f(R)-type theories and k-essence-type theories. In addition to being a scalar-tensor theory, the theory depends on both R and Φ and also includes a kinetic term ($X = \frac{1}{2}\partial_\mu\Phi\partial^\mu\Phi$). For this reason, it is a theory with a high chance of success in examining expansion periods of the Universe and the evolution of Λ-CDM. In addition, f(R,Φ,X) theory is defined both Einstein-frame and Jordan-frame.

f(R,Φ,X) theory action integral is defined as:

$$S = \int \sqrt{-g}\left[\frac{f(R, \Phi, X)}{2\kappa^2} + L_m\right] d\Omega \tag{1}$$

where it can be chosen as $2\kappa^2 = 1$ for simplicity [19, 20]. L_m is a matter part of the Lagrangian function. Considering equation (1), field equations are found as follows:

$$FG_{\mu\nu} - \frac{1}{2}(f(R, \Phi, X) - RF)g_{\mu\nu} + \nabla_\mu \quad \nabla_\nu \quad F + g_{\mu\nu}\nabla_\alpha \quad \nabla^\alpha \quad F - \frac{\epsilon}{2}\Upsilon\nabla_\mu \quad \Phi\nabla_\nu \quad \Phi = T_{\mu\nu} \tag{2}$$

where $F = \frac{\partial f(R,\Phi,X)}{\partial R}$, $\Upsilon = \frac{\partial f(R,\Phi,X)}{\partial X}$ and ϵ is a value corresponding to canonical structure of scalar field [20]. $\epsilon = 1$ was chosen in canonical structure for this study. In f(R,Φ,X) theory, Klein–Gordon equation given as

$$\nabla_\mu(\Upsilon\partial^\mu\Phi) + \epsilon N = 0 \tag{3}$$

where $N = \frac{\partial f(R,\Phi,X)}{\partial \Phi}$ [19]. Energy-momentum tensor of cosmic matter is defined as

$$T_{\mu\nu} = -\frac{2}{\sqrt{-g}}\frac{\delta(\sqrt{-g}L_m)}{\delta(g^{\mu\nu})}. \tag{4}$$

Considering equation (2), Einstein tensor is related with effective energy-momentum tensor ($T^{eff}_{\mu\nu}$), is defined as follows

$$G^{eff}_{\mu\nu} \equiv T^{eff}_{\mu\nu} = \frac{1}{F}(T^c_{\mu\nu} + T_{\mu\nu}). \tag{5}$$

Energy-momentum tensor of curvature in equation (6) is defined as

$$T^c_{\mu\nu} = \frac{1}{2}(f(R, \Phi, X) - RF)g_{\mu\nu} + \nabla_\mu \quad \nabla_\nu \quad F - g_{\mu\nu}\nabla_\alpha \quad \nabla^\alpha \quad F + \frac{\epsilon}{2}\Upsilon\nabla_\mu \quad \Phi\nabla_\nu \quad \Phi. \tag{6}$$

3. General fluid with neutrino in f(R,Φ,X) gravity

Homogeneous and anisotropic Kantowski-Sachs space-time is given by

$$ds^2 = -dt^2 + A^2(t)dr^2 + B^2(t)[d\theta^2 + \sin^2(\theta)d\phi^2] \tag{7}$$

where A and B are metric potentials depend on cosmic time. The anisotropic yet homogeneous structure of Kantowski-Sachs space-time provides an appropriate geometric setting for studying early-universe models that involve spatial curvature and directional stresses. Such a geometry naturally accommodates cosmological scenarios with bulk viscous effects and supports the investigation of isotropization processes over time. These features align with the physical characteristics required in our model and allow the space-time to capture the essential anisotropic dynamics without the need to impose strict planar symmetry or spatial flatness. Ricci curvature scalar for equation (1) is obtained as

$$R = \frac{4ABB''}{AB^2} + \frac{2AB'^2}{AB^2} + \frac{2A''B^2}{AB^2} + \frac{4A'BB'}{AB^2} + \frac{2A}{AB^2} \tag{8}$$

where prime represents partial derivative according to time coordinate. At this point, we firstly consider general diagonal fluid dynamics. Energy-momentum tensor of the fluid can be given as

$$T^\nu_{\mu(fluid)} = diag[T^0_0, T^1_1, T^2_2, T^3_3]. \tag{9}$$

From equations (2)–(6) and (7), components of the Einstein tensor become

$$G^0_0{}_{(eff)} = -\frac{B'^2}{B^2} - \frac{2A'BB'}{AB^2} - \frac{1}{B^2}, \tag{10}$$

$$G^1_1{}_{(eff)} = -\frac{B'^2}{B^2} - \frac{2BB''}{B^2} - \frac{1}{B^2}, \tag{11}$$

$$G^2_2{}_{(eff)} = G^3_3{}_{(eff)} = -\frac{A'B'}{AB} - \frac{AB''}{AB} - \frac{A''B}{AB}. \tag{12}$$

Also, from equations (2)–(6) and (7), components of effective energy-momentum tensor are obtained as

$$T^0_0{}_{(eff)} = \frac{A''}{2A} + \frac{B''}{B} + \frac{3F''}{4F} + \frac{B'^2}{2B^2} + \frac{A'B'}{AB} - \frac{B'F'}{2FB} - \frac{A'F'}{4FA} + \frac{3\epsilon\Upsilon\Phi'^2}{8F} + \frac{1}{2B^2} + \frac{1}{4F}(3T^0_0 + T^1_1 + T^2_2 + T^3_3), \tag{13}$$

$$T^1_{1\ (eff)} = -\frac{A''}{2A} - \frac{B''}{B} + \frac{F''}{4F} - \frac{B'^2}{2B^2} - \frac{A'B'}{AB} + \frac{B'F'}{2FB} - \frac{3A'F'}{4FA} + \frac{\epsilon\Upsilon\Phi'^2}{8F} - \frac{1}{2B^2} + \frac{1}{4F}(T^0_0 + 3T^1_1 - T^2_2 - T^3_3), \tag{14}$$

$$T^2_{2\ (eff)} = -\frac{A''}{2A} - \frac{B''}{B} + \frac{F''}{4F} - \frac{B'^2}{2B^2} - \frac{A'B'}{AB} - \frac{B'F'}{2FB} + \frac{A'F'}{4FA} + \frac{\epsilon\Upsilon\Phi'^2}{8F} - \frac{1}{2B^2} + \frac{1}{4F}(T^0_0 - T^1_1 + 3T^2_2 - T^3_3), \tag{15}$$

$$T^3_{3\ (eff)} = -\frac{A''}{2A} - \frac{B''}{B} + \frac{F''}{4F} - \frac{B'^2}{2B^2} - \frac{A'B'}{AB} - \frac{B'F'}{2FB} + \frac{A'F'}{4FA} + \frac{\epsilon\Upsilon\Phi'^2}{8F} - \frac{1}{2B^2} + \frac{1}{4F}(T^0_0 - T^1_1 - T^2_2 + 3T^3_3). \tag{16}$$

From equations (1)–(3) and (7), for given space-time, Klein–Gordon equation becomes:

$$-\Upsilon'\Phi' + \Upsilon(-\Phi'' - \frac{A'\Phi'}{A} - \frac{2B'\Phi'}{B}) + \epsilon N = 0. \tag{17}$$

It is known that many inflation models have been proposed in the last half-century. Some of the studies envisaged the addition of scalar field. In this way, inflation models can be created without directly considering scalar field in the geometric part of the action, such as Starobinsky-like model of f(R) theory. Starobinsky-like model depends on scalar field and Ricci scalar in a non-minimal way. One of the proposed successful models, $R + R^2$ inflation model,agrees with CMB observations [25–28]. The model is given general form as

$$f_1(R) = R + \alpha R^2 \tag{18}$$

where α is a free parameter related to cosmic expansion with appropriate dimensions [25]. The function doesn't include scalar field, directly. But it receives inflation caused by the scalar fields. On the other hand, k-essence functions allow to define scalar field in action integration, directly. These scalar fields can be canonical or non-canonical (phantom field). This is determined by the η parameter. In this study, canonical scalar fields are used. In accordance with the literature $\Upsilon = \frac{\partial f(R,\Phi,X)}{\partial X} = C_0\eta X^{\eta-1}$ and $X \propto \Phi_{,\alpha}\Phi^{,\alpha}$.

$$f_2(\Phi, X) = C_0 X^{\eta} - 2V(\Phi) \tag{19}$$

here C_0 and X^{η} are arbitrary constants and in the canonical case, it can be chosen as $V(\Phi) = 0$ [21, 29]. In this study, we use a hybrid function that includes both features of f(R) and k-essence functions such as:

$$f(R, \Phi, X) = f_1(R) + f_2(\Phi, X). \tag{20}$$

The specific choice of the function $f(R, \Phi, X) = f_1(R) + f_2(\Phi, X)$ was made to construct a controlled and physically interpretable hybrid model. This form allows the unification of Starobinsky-like inflationary dynamics [25] with scalar field contributions such as k-essence [24]. Although more general formulations including mixed terms are theoretically allowed within the $f(R, \Phi, X)$ framework [30], they typically lead to highly coupled and nonlinear field equations. Such complexity complicates analytical treatment and obscures the underlying physical mechanisms. In contrast, the chosen separable form simplifies the equations and makes it possible to derive exact solutions while still capturing key features of both early and late-time cosmology. Furthermore, it remains consistent with various inflationary and dark energy models widely discussed in the literature [31, 32]. From equations (2), (7)–(9), (18)–(20), field equations are found as follows:

$$-\frac{3\epsilon\Upsilon\Phi'^2}{8} - \frac{A''F}{2A} - \frac{3F''}{4} + \frac{B'^2F}{2B^2} + \frac{B'F'}{2B} + \frac{A'F'}{4A} + \frac{F}{2B^2} - \frac{B''F}{B} + \frac{A'B'F}{AB} = \frac{1}{4}(3T^0_0 + T^1_1 + T^2_2 + T^3_3), \tag{21}$$

$$-\frac{\epsilon\Upsilon\Phi'^2}{8} + \frac{A''F}{2A} - \frac{F''}{4} - \frac{B'^2F}{2B^2} - \frac{B'F'}{2B} + \frac{3A'F'}{4A} - \frac{F}{2B^2} - \frac{A^2B''F}{B} + \frac{A'B'F}{AB} = \frac{1}{4}(T^0_0 + 3T^1_1 - T^2_2 - T^3_3), \tag{22}$$

$$-\frac{\epsilon\Upsilon\Phi'^2}{8} - \frac{A''F}{2A} - \frac{F''}{4} + \frac{B'^2F}{2B^2} + \frac{B'F'}{2B} - \frac{A'F'}{4A} + \frac{F}{2B^2} = \frac{1}{4}(T^0_0 - T^1_1 + 3T^2_2 - T^3_3), \tag{23}$$

$$-\frac{\epsilon\Upsilon\Phi'^2}{8} - \frac{A''F}{2A} - \frac{F''}{4} + \frac{B'^2F}{2B^2} + \frac{B'F'}{2B} - \frac{A'F'}{4A} + \frac{F}{2B^2} = \frac{1}{4}(T^0_0 - T^1_1 - T^2_2 + 3T^3_3). \tag{24}$$

As is commonly known in the literature, if the shear scalar is proportional to scalar expansion for Kantowski-Sachs space-time, metric potential becomes $A = B^m$, $m \neq 1$ [33]. This form is often used in anisotropic cosmological models to establish a connection between the directional scale factors. The proportionality between these factors is physically motivated by the condition that the shear scalar is proportional to the expansion scalar, a well-known assumption in anisotropic geometries that simplifies the description of isotropization processes. From field equations given in equations (21)–(24) and Klein–Gordon equation given in equation (17), we have following solutions set

$$A(t) = n^m(at + b)^{mk}, \tag{25}$$

$$B(t) = n(at + b)^k, \tag{26}$$

$$\Phi(t) = \Phi_0\, t^h, \tag{27}$$

$$F(t) = \frac{4(a + b)^{2(1-k)} + (((4m^2 + 8m + 12)k^2 + (-4m - 8)k + t^2)a^2 + 2abt + b^2)n^2}{(at + b)^2 n^2}, \tag{28}$$

$$\Upsilon(t) = -\Phi_0^{2(\eta-1)} C_1 \eta h^{2(\eta-1)} t^{2(\eta-1)(h-1)}, \tag{29}$$

$$N(t) = -\frac{C_1\eta(\Phi_0 t^{h-1}h)^{2\eta}((h - 1)(2\eta - 1) + k(2 + m))at^{1-h} + 2b(h - 1)t^{-h}(\eta - \frac{1}{2})}{\Phi_0 h\epsilon(at + b)}, \tag{30}$$

where a, b, n, m, k are metric potential constants, Φ_0, h, η, C_1 are constants determining the scalar field behavior, and ϵ are arbitrary constants. In equation (27), the power-law form $\Phi(t) = \Phi_0 t^h$ for the scalar field is not assumed arbitrarily but emerges as a consistent solution of the field equations within the chosen model. This behavior naturally links the dynamics of the scalar field to the structure of the modified gravity framework under consideration. The monotonic time dependence of Φ reflects the interaction between the scalar field and the geometric sector. Also, components of effective energy-momentum tensor are obtained in the following form:

$$\begin{aligned} T_0^0 = {}& \frac{1}{2(at + b)^4 n^4}(24a^2(-1 + (m - 1)k)kn^2(at + b)^{2-2k} + (\epsilon C_1\eta n^4(\Phi_0 h)^{2\eta} t^{(2h-2)\eta}(at + b)^4 \\ & -8\left(\left(\left((m^4 + m^3 + m^2 - 3m)k^3 + (-2m^3 - 2m^2 + m + 3)k^2 + \left(\frac{t^2}{4}(m^2 + m) + 7m^2 + 13m + 16\right)k\right.\right.\right. \\ & \left.\left.\left. -12 - 6m - \frac{t^2}{4}(1 + m)\right)a^2 + \frac{(b^2 + 2abt)}{4}((m^2 - m)k - m - 1)\right)a^2kn^4\right) + 8(at + b)^{-4k+4}\Big) - \tilde{P}(t), \end{aligned} \tag{31}$$

$$\begin{aligned} T_1^1 = {}& \frac{1}{(at + b)^4 n^4}(-12a^2(-1 + (m + 1)k)kn^2(at + b)^{2-2k} - 4(at + b)^{4-4k} \\ & -4((at + b)^{4-2k} + 4a^2n^2(((m^3 + 4m^2 + 7m + 6)k^3 - (4m^2 + 10m + 13)k^2 \\ & \left.\left.\left. + \frac{(t^2 + 12)(m + 2)k - t^2}{4}\right)a^2 + \frac{(b^2 + 2abt)(-1 + (m + 2)k)}{4}\right)k\right)n^2\Big) + \tilde{P}(t), \end{aligned} \tag{32}$$

$$T_2^2 = T_3^3 = \tilde{P}(t) \tag{33}$$

In here, $\tilde{P}(t)$ signs a function related to a dynamical component of general fluid matter. The obtained solutions are given in equations (31)–(33), show that energy-momentum tensor can be considered general fluid matter depend on bulk viscous fluid with neutrino such as

$$\begin{aligned} T^{\nu}_{\mu(fluid)} &= T^{\nu}_{\mu(BulkViscousFluid)} + T^{\nu}_{\mu(Neutrino)} \\ &= diag[P_R, P_\theta, P_\phi, -\rho] + diag[\chi, 0, 0, -\chi]. \end{aligned} \tag{34}$$

In here, components of the tensor for neutrino obtained from $T_{\mu\nu} = \chi\ell_\mu\ell_\nu$, in which $\ell_\mu\ell^\nu = 1$ and $\ell_\mu u^\nu = 0$. χ represents neutrino tension. In the present work, no explicit coupling between the neutrinos and the scalar field is considered, and χ is treated as a phenomenological parameter describing the tension associated with the neutrino flux. From equations (31)–(34), we obtained energy density, radial pressure, viscosity contribution of fluid and tension of neutrino in the following form:

$$\begin{aligned} \rho = {}& \frac{1}{2(at + b)^4 n^4(1 - \omega_1 + 2\omega_2)}(\Phi_0^{2\eta} t^{(2h-2)\eta} h^{2\eta}\epsilon\eta n^4 C_1(at + b)^4 \\ & + (12a^2kn^2(mk - 1) + n^2(at + b)^2 + 4(at + b)^{2-2k})4(at + b)^{2-2k} \\ & + (((-2m^4 - 4(m^3 - m^2 + m) + 6)8k^4 + (3m^3 + 4m^2 + m - 8)16k^3 \\ & + ((t^2 + 20)(1 - m^2) - 32m)4k^2 + (24 + (t^2 + 12)m)4k)a^4 + ((-m^2t + t)k^2 \\ & + kmt)8a^3b + ((-m^2 + 1)k^2 + km)4a^2b^2)n^4), \end{aligned} \tag{35}$$

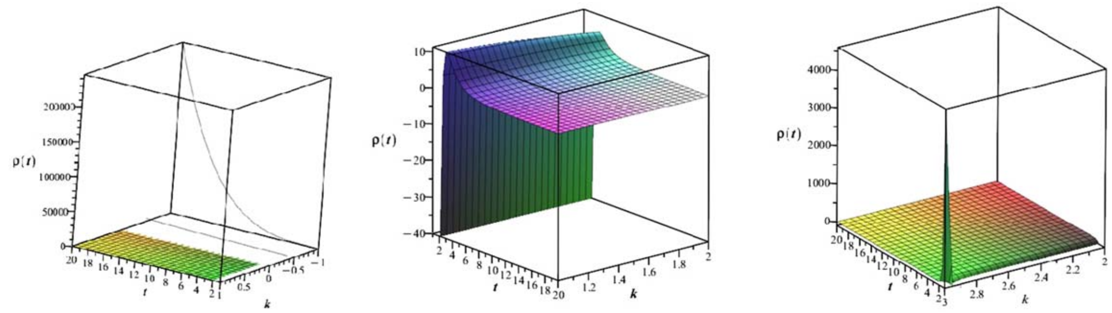

(a) $\rho : -1 < k < 1$ (b) $\rho : 1 < k < 2$ (c) $\rho : 2 < k < 3$

Figure 1. $\rho\,(1 < t < 20, \eta = 2, h = -1, \Phi_0 = C_1 = \epsilon = a = b = 1, \omega_1 = \frac{2}{3}, \omega_2 = \omega_3 = \frac{1}{3}, n = \left(\frac{3}{k(m+2)}\right)^k, m = 2)$.

$$
\begin{aligned}
P_R = {}& \frac{\omega_1}{2(at+b)^4 n^4 (1-\omega_1+2\omega_2)} (\Phi_0^{2\eta} t^{(2h-2)\eta} h^{2\eta} \epsilon\eta n^4 C_1 (at+b)^4 \\
&+ (12a^2kn^2(mk-1) + n^2(at+b)^2 + 4(at+b)^{2-2k})4(at+b)^{2-2k} \\
&+ (((-2m^4 - 4(m^3 - m^2 + m) + 6)8k^4 + (3m^3 + 4m^2 + m - 8)16k^3 \\
&+ ((t^2+20)(1-m^2) - 32m)4k^2 + (24 + (t^2+12)m)4k)a^4 + ((-m^2t + t)k^2 \\
&+ kmt)8a^3b + ((-m^2+1)k^2 + km)4a^2b^2)n^4),
\end{aligned} \tag{36}
$$

$$
\begin{aligned}
P_\theta = P_\Phi = \tilde{P}(t) = {}& \frac{\omega_2}{2(at+b)^4 n^4 (1-\omega_1+2\omega_2)} (\Phi_0^{2\eta} t^{(2h-2)\eta} h^{2\eta} \epsilon\eta n^4 C_1 (at+b)^4 \\
&+ (12a^2kn^2(mk-1) + n^2(at+b)^2 + 4(at+b)^{2-2k})4(at+b)^{2-2k} \\
&+ (((-2m^4 - 4(m^3 - m^2 + m) + 6)8k^4 + (3m^3 + 4m^2 + m - 8)16k^3 \\
&+ ((t^2+20)(1-m^2) - 32m)4k^2 + (24 + (t^2+12)m)4k)a^4 + ((-m^2t + t)k^2 \\
&+ kmt)8a^3b + ((-m^2+1)k^2 + km)4a^2b^2)n^4),
\end{aligned} \tag{37}
$$

$$
\begin{aligned}
\chi = {}& \frac{1}{2(at+b)^4 n^4 (1-\omega_1+2\omega_2)} (\Phi_0^{2\eta}\, t^{(2h-2)\eta} h^{2\eta} \epsilon\eta n^4 C_1 (\omega_2 - \omega_1)(at+b)^4) \\
&- 48n^2\left(\left(\left(\frac{1}{2}(1 + (\omega_1+1)m - \omega_1 + 2\omega_2)\right)k^2 - \frac{1}{2}(\omega_1+1)k + \frac{t^2\omega_2}{12}\right)a^2 + \frac{\omega_2}{12}(b^2 + 2abt)\right) \\
&\times (at+b)^{2-2k} + 2n^2(2\omega_2 - (\omega_1+1))(at+b)^{4-2k} \\
&+ \left(\frac{n^4a^2b^2k}{8} + \frac{abt}{4}\right)(((\omega_1+1)m + 2\omega_2 + 2)(m-1)k - (\omega_1+1)m + (1-\omega_1) + 2\omega_2) \\
&+ 16\left(\left((m-1)k^2\left((m^2+2m+3)\left(\frac{1}{2}(\omega_1+1)m + \omega_2 + 1\right) - ((\omega_1+\omega_2+2)m^2\right.\right.\right. \\
&+ (2\omega_1 + 3\omega_2 + 5)m + \omega_2 + 1)) + \left(\left(\frac{1}{2}\left(3 + \frac{t^2}{4}(\omega_1+1) + 7\omega_1 - 4\omega_2\right)\right)m^2\right. \\
&\left. + \frac{1}{2}(3 + \frac{t^2}{4}(1 - \omega_1 + 2\omega_2) + 13\omega_1 - 10\omega_2) + 8\omega_1 - \frac{t^2}{4} - 11\omega_2 - 3\right)k \\
&\left.\left. + 3(\omega_2 - \omega_1)(m+2) - \frac{t^2}{8}((\omega_1+1)m - 1 - 2\omega_2 + \omega_1)\right)a^2k - 8(\omega_1+1)(at+b)^{4-4k}\right)
\end{aligned} \tag{38}
$$

where $diag[P_R, P_\theta, P_\phi, -\rho] = diag[\omega_1, \omega_2, \omega_3, -1]\rho$ and ω_i denotes the directional equation of state parameters along each spatial direction in the anisotropic Kantowski-Sachs geometry. It is seen from equation (36) that ω_2 and ω_3 are obtained as equal to each other.

The evolution of ρ with time and the constant k is graphed in figure 1. In figure 1, it is obtained the density time graph for three different k values. As can be seen in the graphs, the k value has an effect on whether the density is positive or negative. In figure 1(a), density takes positive values when the k value is between 0 and 1. When the value of k is negative, density is in the positive area only for the values of -0.5 and -1. In figure 1(b), at the beginning of time, the density always takes negative values. When density reaches positive values, it has a maximum then decreases with time and approaches zero. In figure 1(c), as the k value approaches 3, the density takes positive values. While it has a maximum value at the beginning of time, the density decreases over time.

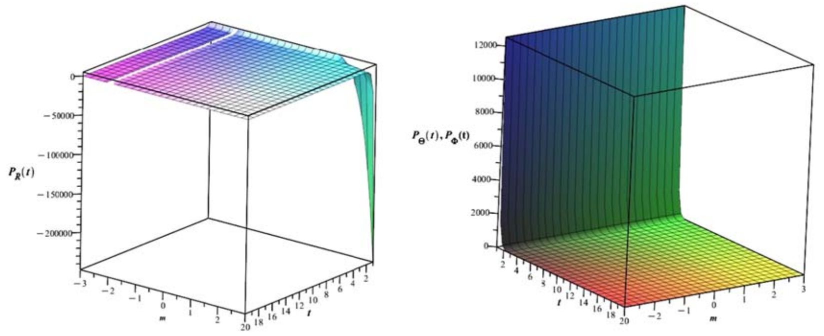

(a) $P_R : -3 < m < 3$ (b) $P_\theta = P_\phi : -3 < m < 3$

Figure 2. P_R and $P_\theta = P_\phi$ $(1 < t < 20, \eta = 2, h = -1, \Phi_0 = C_1 = \epsilon = a = b = 1, \omega_1 = \frac{2}{3}, \omega_2 = \omega_3 = \frac{1}{3}, n = \left(\frac{3}{k(m+2)}\right)^k, k = 3)$.

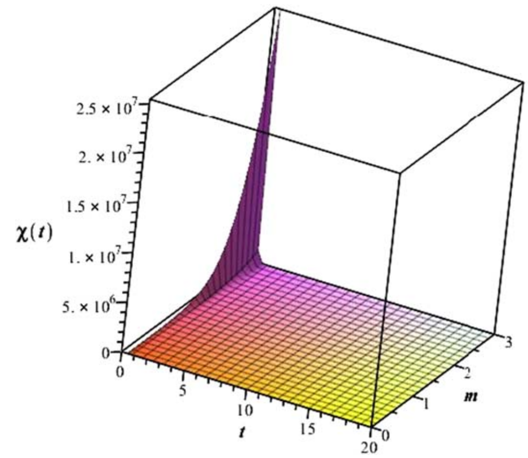

Figure 3. *Neutrino* $(0 < t < 20, 0 < m < 3, \eta = 2, h = -1, \Phi_0 = C_1 = \epsilon = a = b = 1, \omega_1 = \frac{2}{3}, \omega_2 = \frac{1}{3}, n = \left(\frac{3}{k(m+2)}\right)^k, k = 3)$.

The evolution of P_R, P_θ and P_ϕ with time and the constant m is graphed in figure 2. In figure 2, P_R has a maximum at the beginning of time but it has negative values when m approaches 3. For other choices of m, P_R is decreases with time and approaches zero. Also, it has a singular point around $m = 2.5$. For P_θ and P_ϕ, they have a maximum at the beginning of time and then approach zero with time, as well.

The evolution of Neutrino tension, χ with time and the constant m is graphed in figure 3. It is seen that neutrino tension has a maximum in the beginning when m approaches to 3. The neutrino tension decreases both with time and as the m approaches zero.

The volume scale factor for the Kantowski-Sachs spacetime relationship between them is defined as follows:

$$V = S^3 = AB^2 = n^{m+2}(at + b)^{(m+2)k} \tag{39}$$

where S is the average of the scale factor and A, B are metric potentials. Scale factor:

$$S = (AB^2)^{\frac{1}{3}} = (n^{m+2}(at + b)^{(m+2)k})^{\frac{1}{3}} \tag{40}$$

As it is known, the average Hubble parameter is given as follows:

$$H = \frac{S'}{S} = \frac{1}{3}(H_1 + H_2 + H_3) = \frac{1}{3}\left(\frac{A'}{A} + 2\frac{B'}{B}\right) = \frac{a(m+2)k}{3(at+b)} \tag{41}$$

H_1, H_2 and H_3 indicate directional Hubble parameters along axes. Directional Hubble parameters for Kantowski-Sachs space-time are taken as $H_1 = \frac{A'}{A}$ and $H_2 = H_3 = \frac{B'}{B}$. As it is known, that scalar expansion, sheer scalar and anisotropy parameters are given as follows, respectively:

$$\Theta = 3H = \frac{1}{3}\left(\frac{A'}{A} + 2\frac{B'}{B}\right) = \frac{a(m+2)k}{at+b} \tag{42}$$

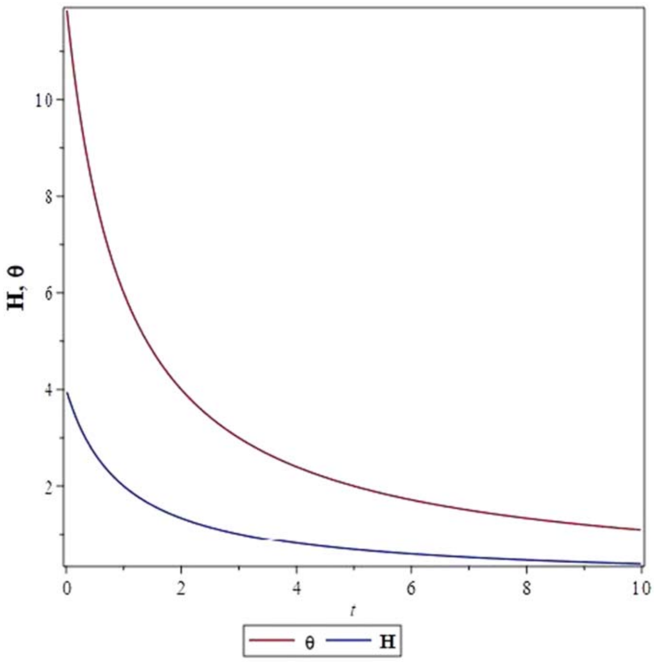

Figure 4. H and Θ $(0 < t < 10, \eta = 2, h = -1, \Phi_0 = C_1 = \epsilon = a = b = 1, \omega_1 = \frac{2}{3}, \omega_2 = \frac{1}{3}, n = \left(\frac{3}{k(m+2)}\right)^k, k = 3, m = 2)$.

$$\sigma^2 = \frac{1}{2}\left(H_i^2 - \frac{\Theta^2}{3}\right) = \frac{1}{3}\left(\frac{A'^2}{A} + 2\frac{B'^2}{B} - 2\frac{A'B'}{AB} - \frac{B'^2}{B^2}\right) = \frac{a^2(m-1)^2k^2}{3(at+b)^2} \tag{43}$$

$$\Delta = \frac{1}{3}\sum_{i=1}^{3}\left(\frac{H_i - H}{H}\right)^2 = 0 \tag{44}$$

where, H_i is directional Hubble parameters. Taking into account the average of the scale factor given by equation (40), the deceleration parameter is defined as follows:

$$q = -\frac{SS''}{S'^2} = \frac{d}{dt}\left(\frac{1}{H}\right) - 1 = \frac{3-(m+2)k}{(m+2)k} \tag{45}$$

The deceleration parameter (q) provides us with various explanations about expanding universe; A positive q indicates a slowing down phase, while a negative q indicates the acceleration phase of the Universe. The evolution of the Hubble parameter and scalar expansion for some selection of constants are represented in figure 4. Hubble parameter and scalar expansion have a maximum at the beginning of time and then approach zero with time. Also, the deceleration parameter is attained as $q = -3/4$ for the same selection of constant in the solutions. This interval describes a physically realistic regime supported by current cosmological observations, where the expansion is accelerating but not dominated by a pure cosmological constant. Therefore, the choice of $q = -\frac{3}{4}$ in the present model reflects a scenario compatible with this observationally favored range, providing a consistent description of cosmic acceleration. Also, Hubble parameter and deceleration parameter are examined together, they reflects a cosmological model in which the Universe is expanding at an accelerating rate in the beginning and then it reaches a state where its expansion slows to a halt, leading to a potentially static or contracting future. Shear scalar for the constructed model is positive and it approaches zero with time. It can be related that space-time is passing from an anisotropic expansion to a more isotropic state. At the same time, the anisotropy parameter is obtained as zero. It means that the constructed model has become isotropic at the current or final stage of it.

In the study of space-time geometry, energy conditions play a crucial role in understanding the physical implications of gravitational theories. These conditions, which are derived from the properties of matter and energy, help to determine the possible structures of space-time and the behavior of gravitational fields. Energy conditions impose restrictions on the stress-energy tensor, which describes the distribution and flow of energy and momentum. By analyzing these conditions, it is possible to gain insights into the nature of singularities, the stability of space-time configurations, and the viability of various cosmological models. In the presence of perfect fluid in the effective gravitational field, the energy conditions are classified depending on effective pressures and effective density. By using equations (13)–(16) with equations (25)–(30), one gets effective components of an energy-momentum tensor as follows:

$$\begin{aligned}\rho^{eff} &= 16\left(\left((m^2+6m+5)k^2+(-2-m)k+\frac{t^2}{4}\right)a^2+\frac{bta}{2}+\frac{b^2}{4}\right)(at+b)^2n^4\\&\times\left(\left((m^2+2m+3)k^2+(-2-m)k+\frac{t^2}{4}\right)a^2+\frac{bta}{2}+\frac{b^2}{4}\right)(at+b)^{2k}+32k^2a^2\left(m+\frac{1}{2}\right)n^6\\&\times\left(\left((m^2+2m+3)k^2+(-2-m)k+\frac{t^2}{4}\right)a^2+\frac{bta}{2}+\frac{b^2}{4}\right)^2(at+b)^{4k}\\&+32(at+b)^4\left(\frac{(at+b)^{2-2k}}{2}+n^2\left(\left(\left(m^2+3m+\frac{7}{2}\right)k^2+(-2-m)k+\frac{t^2}{4}\right)a^2\right.\right.\\&\left.\left.+\frac{bta}{2}+\frac{b^2}{4}\right)\right)/16\left(n^2\left(\left((m^2+2m+3)k^2+(-2-m)k+\frac{t^2}{4}\right)a^2+\frac{bta}{2}+\frac{b^2}{4}\right)(at+b)^{2k}\right.\\&+(at+b)^2)^2(at+b)^2n^2\end{aligned} \tag{46}$$

$$\begin{aligned}P_R^{eff} &= -16\left(\left((m^2+2m+9)k^2+(-6-m)k+\frac{t^2}{4}\right)a^2+\frac{bta}{2}+\frac{b^2}{4}\right)(at+b)^2n^4\\&\times\left(\left((m^2+2m+3)k^2+(-2-m)k+\frac{t^2}{4}\right)a^2+\frac{bta}{2}+\frac{b^2}{4}\right)(at+b)^{2k}-48ka^2n^6\\&\times\left(\left((m^2+2m+3)k^2+(-2-m)k+\frac{t^2}{4}\right)a^2+\frac{bta}{2}+\frac{b^2}{4}\right)^2\left(k-\frac{2}{3}\right)(at+b)^{4k}\\&-32(at+b)^4\left(\frac{(at+b)^{2-2k}}{2}+n^2\left(\left(\left(m^2+2m+\frac{9}{2}\right)k^2+(-m-3)k+\frac{t^2}{4}\right)a^2\right.\right.\\&\left.\left.+\frac{bta}{2}+\frac{b^2}{4}\right)\right)/16\left(n^2\left(\left((m^2+2m+3)k^2+(-2-m)k+\frac{t^2}{4}\right)a^2+\frac{bta}{2}+\frac{b^2}{4}\right)(at+b)^{2k}\right.\\&+(at+b)^2)^2(at+b)^2n^2\end{aligned} \tag{47}$$

$$\begin{aligned}P_\theta^{eff} &= P_\Phi^{eff}=-(ka^2((m^2+m+1)k-1)(n^4(((m^2+2m+3)k^2+(-2-m)k\\&+\left.\frac{t^2}{4}\right)a^2+\frac{bta}{2}+\left.\frac{b^2}{4}\right)^2(at+b)^{4k}+2(at+b)^2(n^2(((m^2+2m+3)k^2+(-2-m)k\\&+\left.\frac{t^2}{4}\right)a^2+\frac{bta}{2}+\left.\frac{b^2}{4}\right)(at+b)^{2k}+\left.\left.\left.\frac{(at+b)^2}{2}\right)\right)\right)/16(n^2(((m^2+2m+3)k^2+(-2-m)k\\&+\left.\frac{t^2}{4}\right)a^2+\frac{bta}{2}+\left.\frac{b^2}{4}\right)(at+b)^{2k}+\left.(at+b)^2\right)^2(at+b)^2n^2\end{aligned} \tag{48}$$

The evolution of effective energy-momentum tensor components is represented in figure 5. Effective energy density has a maximum at the beginning of the time and decreases with time. Effective pressure components get negative values in the model. They have a minimum at the beginning of the time and are approaching zero with time. The behavior of all components for effective matter form indicates exotic matter form. In this case, it would be useful to examine the energy conditions for the model constructed by taking into account the effective matter distribution. Energy conditions are classified as null energy condition (NEC), weak energy condition (WEC), dominant Energy Condition (DEC) and Strong Energy Condition (SEC) in the following form:

$$NEC:\ \left\{\rho^{eff}+P_R^{eff}\geqslant 0,\quad \rho^{eff}+P_\theta^{eff}\geqslant 0,\quad \rho^{eff}+P_\Phi^{eff}\geqslant 0.\right. \tag{49}$$

$$WEC:\ \begin{cases}\rho^{eff}\geqslant 0,\\ \rho^{eff}+P_R^{eff}\geqslant 0,\quad \rho^{eff}+P_\theta^{eff}\geqslant 0,\quad \rho^{eff}+P_\Phi^{eff}\geqslant 0.\end{cases} \tag{50}$$

$$DEC:\ \begin{cases}\rho^{eff}\geqslant 0,\\ \rho^{eff}-|P_R^{eff}|\geqslant 0,\quad \rho^{eff}-|P_\theta^{eff}|\geqslant 0,\quad \rho^{eff}-|P_\Phi^{eff}|\geqslant 0.\end{cases} \tag{51}$$

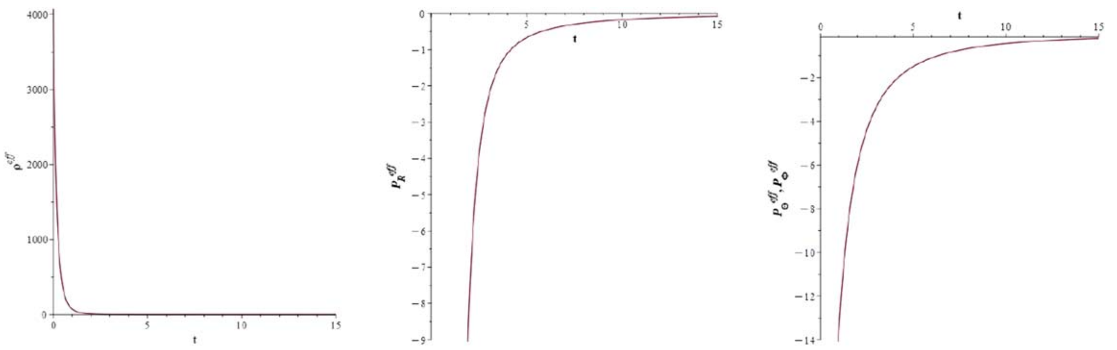

(a) ρ^{eff} (b) P_R^{eff} (c) $P_\theta^{eff} = P_\phi^{eff}$

Figure 5. ρ^{eff}, P_R^{eff}, $P_\theta^{eff} = P_\phi^{eff}$ $(1 < t < 15,\ \eta = 2,\ h = -1,\ \Phi_0 = C_1 = \epsilon = a = b = 1,\ \omega_1 = \frac{2}{3},\ \omega_2 = \frac{1}{3},\ n = \left(\frac{3}{k(m+2)}\right)^k,$ $k = 3,\ m = 2)$.

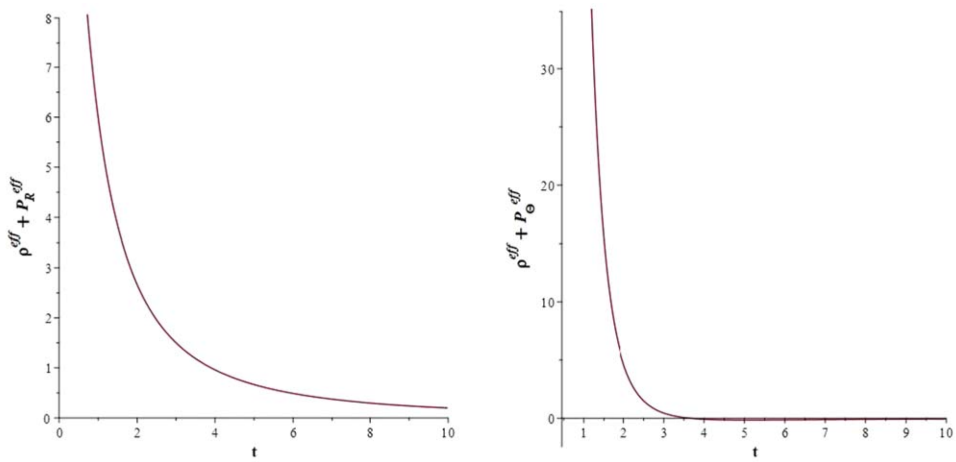

(a) $\rho^{eff} + P_R^{eff}$ (b) $\rho^{eff} + P_\theta^{eff} = \rho^{eff} + P_\Phi^{eff}$

Figure 6. $\rho^{eff} + P_R^{eff}$, $\rho^{eff} + P_\theta^{eff} = \rho^{eff} + P_\Phi^{eff}$ $(1 < t < 10, \eta = 2, h = -1, \Phi_0 = C_1 = \epsilon = a = b = 1,\ \omega_1 = \frac{2}{3},\ \omega_2 = \frac{1}{3},$ $n = \left(\frac{3}{k(m+2)}\right)^k, k = 3, m = 2)$.

$$SEC: \begin{cases} \rho^{eff} + P_R^{eff} \geqslant 0, \quad \rho^{eff} + P_\theta^{eff} \geqslant 0, \quad \rho^{eff} + P_\Phi^{eff} \geqslant 0, \\ \rho^{eff} + P_R^{eff} + P_\theta^{eff} + P_\Phi^{eff} \geqslant 0. \end{cases} \tag{52}$$

By using equations (46)–(52), we represented the evolution of energy conditions with time in figures 6, 7 and 8. In figure 6, NEC is satisfied for all components of effective energy momentum tensor. It has a maximum at the beginning of the time and approaches zero with time. In figure 1(c), it is seen that the effective energy density has a positive value in the case of $f = 3$. If we consider figures 1(c) and 5, they indicate that WEC is satisfied for the constructed model, as well. Also, DEC is satisfied by considering figures 1(c) and 7 together. It is seen that all the conditions that must be met have a maximum and then approach zero. In figure 8, SEC is represented and $\rho^{eff} + P_R^{eff} + P_\theta^{eff} + P_\Phi^{eff}$ condition is violated for constructed model. It means that the gravitational field produced by a distribution of matter can lead to a scenario where gravity repels matter in a way that would allow for certain exotic configurations.

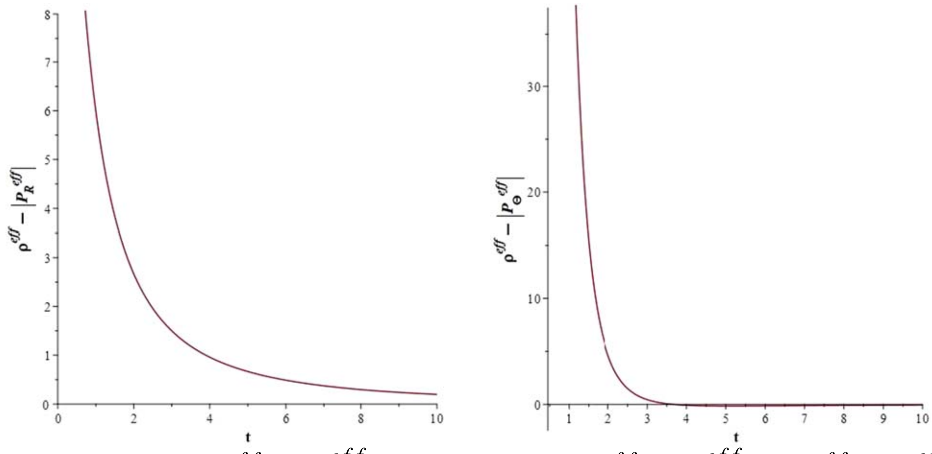

(a) $\rho^{eff} - \mid P_R^{eff} \mid$ (b) $\rho^{eff} - \mid P_\theta^{eff} \mid = \rho^{eff} - \mid P_\Phi^{eff} \mid$

Figure 7. $\rho^{eff} - |P_R^{eff}|$, $\rho^{eff} - |P_\theta^{eff}| = \rho^{eff} - |P_\Phi^{eff}|$ $(1 < t < 10, \eta = 2, h = -1, \Phi_0 = C_1 = \epsilon = a = b = 1, \omega_1 = \frac{2}{3}, \omega_2 = \frac{1}{3}, n = \left(\frac{3}{k(m+2)}\right)^k, k = 3, m = 2)$.

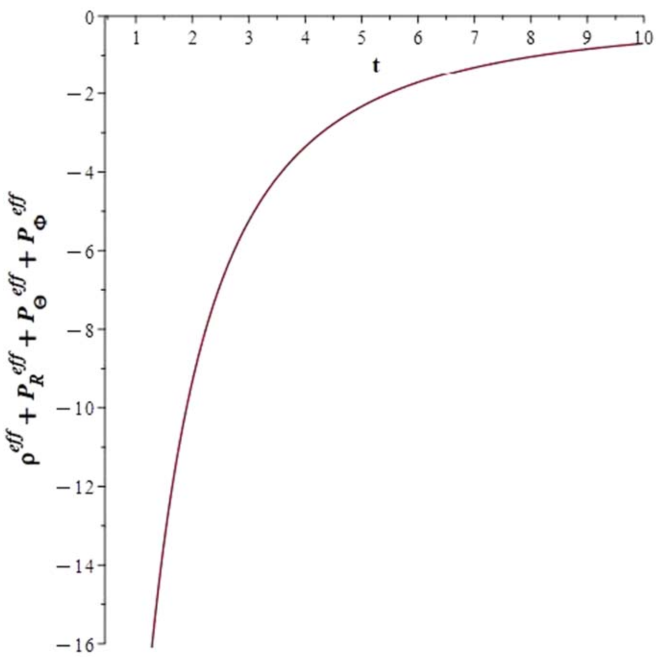

Figure 8. $\rho^{eff} + P_R^{eff} + P_\theta^{eff} + P_\Phi^{eff}$ $(1 < t < 10, \eta = 2, h = -1, \Phi_0 = C_1 = \epsilon = a = b = 1, \omega_1 = \frac{2}{3}, \omega_2 = \frac{1}{3}, n = \left(\frac{3}{k(m+2)}\right)^k, k = 3, m = 2)$.

4. Conclusion

In this study, we investigate Kantowski-Sachs space-time in the presence of general fluid distribution in f(R,Φ,X) gravity. The field equation of the model is constructed under the consideration of the hybrid f(R,Φ,X) function including the Starobinsky-like model and k-essence function with canonical scalar fields. Under those assumptions, we obtain solutions to the field equations. The obtained solutions in f(R,Φ,X) gravity sign that considered general fluid could be viscous fluid with neutrinos. All unknown quantities are obtained for the constructed model. In f(R,Φ,X) theory, the scalar field given by equation (27), is obtained as a function of time. It has a maximum at the beginning of time and then approaches zero. To get a physically meaningful construction, we analyze the evolution of energy density concerning time and constant, k. It is shown that energy density can get negative values for some selection of constant k. In the case of $2 < k < 3$, energy density has a maximum at the beginning of time and decreases with time and the selection of a smaller constant, k. The solutions indicate that

P_θ and P_ϕ are equal in the fluid. Also, the evolution of P_R, P_θ and P_ϕ with time and the constant, m, are examined for some selection of arbitrary constants. It is shown that P_R has a negative maximum and approaches zero with time, while P_θ and P_ϕ have a maximum and are approaching zero with time. Also, P_R has a singular point, as well. The fluid has attractive behavior in the direction of θ and ϕ, while it has repulsive behavior in the direction of r. The evolution of Neutrino tension is examined for some selection of arbitrary constants. At the beginning of time, Neutrino tension gets maximum value then it gets zero for $t \to \infty$. The fact that the density of neutrinos was high in the early universe and decreased over time may have caused the kinetic energy of the neutrinos to decrease and therefore the energy density to decrease in the event of rapid expansion of space-time on a certain axis. Simultaneously, the shear scalar σ^2 decreases with time indicating isotropization of the space-time geometry. The presence of bulk viscosity further supports this transition by acting as a damping mechanism for anisotropic stresses. While the neutrino flux contributes as an independent energy component in the model, it does not explicitly couple to the viscous sector. Therefore, the damping of anisotropies and the isotropization process are attributed to the viscous effects of the cosmic fluid, which may play a supportive role during the neutrino decoupling era.

For this purpose, we examine the kinematical quantities of the constructed model. In the constructed model, we obtain the Hubble parameter and scalar expansion as a function that takes positive values and then approaches zero for $t \to \infty$. Also, the deceleration parameter is obtained as a negative constant. They reflects a cosmological model in which the Universe is expanding at an accelerating rate in the beginning and then it reaches a state where its expansion slows to a halt, leading to a potentially static or contracting future.

Energy conditions play a crucial role in understanding the physical implications of gravitational theories. Therefore, we analyze effective energy condition of the constructed model to understand the effect of not only the material distribution but also the geometry of the dynamic structure. Effective distractions are attained for the constructed model. In figure 5(a), effective energy density is attained as positive and approaches zero for $t \to \infty$. Also, all components for effective pressures have negative values and approaches to zero for $t \to \infty$. Here it is seen that when the matter distribution and the effect of the theory are taken into account together, the distribution behaves like exotic matter. Energy conditions like NEC, WEC and DEC have maximum positive values and then approach zero for $t \to \infty$, while SEC has a negative maximum and then approaches zero for $t \to \infty$. It means that NEC, WEC and DEC are satisfied while SEC is violated for constructed model. The violation of SEC arises naturally due to the negative effective pressure generated by the bulk viscous fluid and scalar field dynamics. This behavior is consistent with many dark energy models and inflationary scenarios, where the violation of SEC is considered a necessary condition for accelerated expansion [34]. In our solutions, the deceleration parameter remains negative with $q = -\frac{3}{4}$, indicating accelerated expansion, while the Hubble parameter remains positive and decreases over time toward zero. This behavior reflects the SEC violation as a physical requirement for sustaining cosmic acceleration without introducing a cosmological constant.

Acknowledgments

This study is supported by Çanakkale Onsekiz Mart University Scientific Research Projects. Project Number: FBA-2023-4643.

Data availability statement

No new data were created or analysed in this study.

ORCID iDs

Erkan Eraslan https://orcid.org/0000-0002-1741-9399
Melis Ulu Doğru https://orcid.org/0000-0003-1788-3885
Doğukan Taşer https://orcid.org/0000-0002-8622-6830
Hüseyin Aydın https://orcid.org/0000-0002-5471-619X

References

[1] Ellis G F R 1971 *Proc. Int. Sch. Phys. Fermi* **47** 104–82
[2] Misner C W 1968 *Astrophys. J.* **151** 431–57
[3] Banerjee A, Duttachoudhury S B and Sanyal A K 1985 *J. Math. Phys.* **26** 3010–5
[4] Ram S and Singh C P 1997 *Astrophys. Space Sci.* **254** 143–50
[5] Bali R and Upadhaya R D 2003 *Astrophys. Space Sci.* **283** 97–108

[6] Gavassino L, Antonelli M and Haskell B 2021 *Class. Quant. Grav.* **38** 075001
[7] Solanki R, Pacif S K J, Parida A and Sahoo P K 2021 *Phys. Dark Univ.* **32** 100820
[8] Koussour M, Errehymy A, Donmez O, Myrzakulov K, Khan M A, Çil B and Güdekli E 2024 *Physics of the Dark Universe* **45** 101527
[9] Abebe A, Alfedeel A H, Sofuoglu D, Hassan E I and Tiwari R K 2023 *Universe* **9** 61
[10] Çaglar H and Aygün S 2015 *IOSR Journal of Mathematics* **11** 53–9
[11] Lesgourgues J, Mangano G, Miele G and Pastor S 2013 *Neutrino Cosmology* (Cambridge University Press)
[12] Dolgov A D 2002 *Phys. Rept.* **370** 333–535
[13] Hannestad S 2006 *Ann. Rev. Nucl. Part. Sci.* **56** 137–61
[14] Lesgourgues J and Pastor S 2006 *Phys. Rept.* **429** 307–79
[15] Hannestad S 2010 *Prog. Part. Nucl. Phys.* **65** 185–208
[16] Motohashi H, Starobinsky A A and Yokoyama J 2012 *Int. J. Mod. Phys. Conf. Ser.* **10** 35–42
[17] He J h 2013 *Phys. Rev. D* **88** 103523
[18] Hwang J c and Noh H 2002 *Phys. Rev. D* **66** 084009
[19] Tsujikawa S 2007 *Phys. Rev. D* **76** 023514
[20] Bahamonde S, Böhmer C G, Lobo F S N and Sáez-Gómez D 2015 *Universe* **1** 186–98
[21] Oikonomou V K and Chatzarakis N 2020 *Nucl. Phys. B* **956** 115023
[22] Buchdahl H A 1970 *Mon. Not. Roy. Astron. Soc.* **150** 1–8
[23] Hwang J C 1990 *Class. Quant. Grav.* **7** 1613–31
[24] Armendariz-Picon C, Mukhanov V F and Steinhardt P J 2001 2001*Phys. Rev. D* **63** 103510
[25] Starobinsky A A 1980 *Phys. Lett. B* **91** 99–102
[26] Ade P A R *et al* 2016 *Astron. Astrophys.* **594** A20
[27] Cervantes-Cota J L and Dehnen H 1995 *Nucl. Phys. B* **442** 391–412
[28] Barvinsky A O, Kamenshchik A Y and Starobinsky A A 2008 *JCAP* 021
[29] Bronnikov K A, Fabris J C and Rodrigues D C 2020 *Int. J. Mod. Phys. D* **29** 2050016
[30] Nojiri S and Odintsov S D 2007 *Int. J. Geom. Meth. Mod. Phys.* **4** 115–46
[31] Nojiri S and Odintsov S D 2011 *Phys. Rept.* **505** 59–144
[32] Clifton T, Ferreira P G, Padilla A and Skordis C 2012 *Phys. Rept.* **513** 1–189
[33] Collins C B, Glass E N and Wilkinson D A 1980 *Gen. Rel. Grav.* **12** 805–23
[34] Visser M and Barcelo C 2000 *3rd International Conference on Particle Physics and the Early Universe* pp 98–112